Stresses in a Planar Soil Composite in Plane Strain Compression

M. Abramento
Instituto de Pesquisas Tecnológicas, Sao Paulo, Brazil

A. J. Whittle
Massachusetts Institute of Technology, Boston, USA

ABSTRACT: This paper presents an analytical method for estimating the stresses in planar tensile reinforcements due to compressive shearing of the surrounding soil mass. The formulation adapts techniques of shear-lag analysis, commonly used in the mechanics of composites. The analyses assume that the soil and reinforcement behave as linear, isotropic and elastic materials, linked through a frictional interface. The inclusion is oriented parallel to the minor, external, principal stress. Closed form solutions are presented for the axial reinforcement stresses, soil-reinforcement interface tractions and lateral stresses in the soil as functions of inclusion geometry, material properties and boundary stresses. The proposed formulation provides a simple and direct method for estimating the stress distribution within reinforced soil masses at working load conditions.

1 INTRODUCTION

Synthetic materials (steel strips, arrays of fibers, geosynthetic fabrics and grids) are widely used to reinforce soil masses in retaining walls, embankments, foundations and pavements. The performance of these composite soil structures depends mainly on the interaction between the soil and reinforcing inclusions, determining the magnitude of loads carried by the reinforcements. There are three basic approaches used in existing studies of soil-reinforcement interaction: 1) homogenization methods, 2) limit equilibrium calculations, and 3) explicit modeling of the soil matrix and reinforcing inclusions.

Homogenization methods assume that the soil is reinforced with closely spaced inclusions and behaves macroscopically as a homogeneous, anisoptropic composite material (e.g. Harrison and Gerrard, 1972). Homogenization greatly simplifies the representation of soil-reinforcement interaction, but does not consider the effects of inclusion spacing. Current design methods for reinforced soil masses are based primarily on limit equilibrium analyses (e.g. Jewell, 1990). Stability of the structure is maintained either through sliding resistance along the soil-reinforcement interface or through tensile stresses generated in the reinforcement, resisted by a bond or anchor length embedded in the stable soil mass (i.e., pullout mode). Limit equilibrium calculations are not reliable for estimating the magnitude and distribution of reinforcement stresses at working load conditions.

Comprehensive stress analyses for reinforced soil masses can be achieved using finite element methods, explicitly modeling the constitutive properties of the soil, reinforcement and interfaces. These analyses offer great flexibility for simulating complex problem geometries, construction histories, etc. However, it is difficult to interpret the mechanisms controlling soil-reinforcement interaction from complex numerical analyses. This paper summarizes an analytical method for estimating the tensile stresses in a single planar reinforcement due to shearing of the surrounding soil matrix. The analysis expresses reinforcement stresses as closed form functions of the inclusion geometry (thickness, spacing and length), elastic properties of the constituent materials (i.e., soil matrix and reinforcement), interface friction and level of external stresses. The proposed formulation adapts the techniques of shear-lag analysis (Kuhn, 1956) which are commonly used in the mechanics of fiber reinforced composites (e.g. Budiansky et al., 1986).

2 FORMULATION

Figure 1 shows the geometry for a composite plane strain element of reinforced soil considered in this analysis. It comprises a planar inclusion of thickness, f, and length, L, embedded in a soil matrix of overall height, m+f (inclusion spacing). The inclusion is parallel to the minor, external, principal stress on the soil matrix, σ_3.

Compressive stresses are positive in the soil mass while inclusion stresses are positive in tension. The soil is sheared in a plane strain compression mode by

increasing the major principal stress σ_1 (and/or reducing the minor principal stress σ_3). For these loading conditions, the inclusion resists the lateral tensile strains which would otherwise develop in the soil, and therefore represents the optimal orientation for a planar tensile reinforcement.

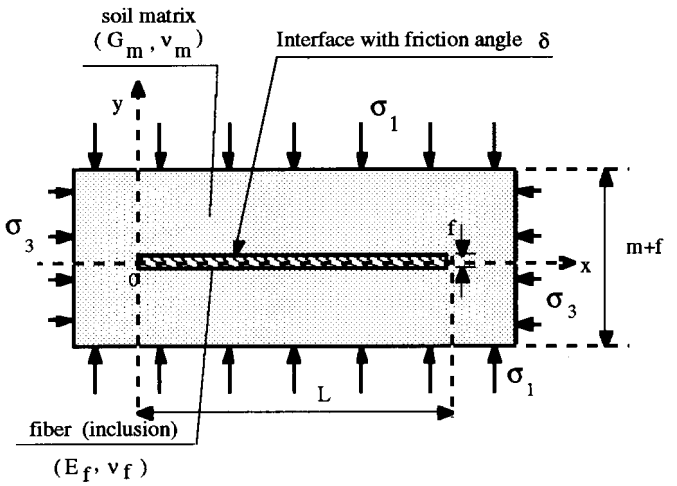

Fig. 1 Geometry for an element of reinforced soil

The stresses to be determined are: a) axial stresses in the inclusion (σ^f_{xx}); b) shear (σ^i_{xy}) and normal (σ^i_{yy}) stresses along the inclusion-matrix interface; and c) axial (σ^m_{xx}), normal (σ^m_{yy}) and shear (σ^m_{xy}) stresses within the soil matrix. The proposed analysis assumes that: 1) The soil matrix and reinforcement behave as linear, isotropic and elastic materials (with properties G_m, ν_m and E_f, ν_f, respectively, Fig. 1). 2) The soil matrix and reinforcing inclusion are linked through a frictional interface (δ; Fig.1). 3) There is no axial stress acting at the ends of the inclusion, (i.e. $\sigma^f_{xx}=0$ at x=0, L) as the inclusion is thin and is not physically bonded to the soil matrix. 4) The axial stresses in the soil matrix and in the inclusion are functions of x only (σ^m_{xx} is the average stress acting in the soil matrix):

$$\overline{\sigma}^m_{xx} = \sigma^m_{xx} = a\,\sigma^f_{xx} + \sigma_3\,(1+a) \qquad (1)$$

where a=f/m is the 'inclusion ratio'.

For practical ranges of soil-reinforcement friction (δ=10°-35°), Abramento and Whittle (1993) have shown that interface slippage has minor influence on the load transferred in plane strain compression. Hence, the tensile stress in the inclusion can be estimated for the case of no interface sliding by:

$$\sigma^f_{xx} = \frac{K_2\sigma}{K_1}\left[1 - \frac{\cosh\sqrt{K_1}\left(\frac{L}{2} - x\right)}{\cosh\sqrt{K_1}\frac{L}{2}}\right] \qquad (2)$$

where:

$$K_2\sigma = K_2^1\,\sigma_1 + K_2^3\,\sigma_3 \qquad (3)$$

and K_1, K_2^1, K_2^3 are constants defined in terms of the material properties and geometry:

$$K_1 = \frac{6}{m\,f}\,\frac{\left[(1-\nu_m)\,a + 2\frac{G_m}{E_f}(1+\nu_f)(1-\nu_f)\right]}{\left[1+\frac{1}{4}\nu_m - \frac{3}{2}\frac{G_m}{E_f}(1+\nu_f)\nu_f\right]} \qquad (3a)$$

$$K_2^1 = \frac{6}{m\,f}\,\frac{\left[\nu_m - 2\frac{G_m}{E_f}(1+\nu_f)\nu_f\right]}{\left[1+\frac{1}{4}\nu_m - \frac{3}{2}\frac{G_m}{E_f}(1+\nu_f)\nu_f\right]} \qquad (3b)$$

$$K_2^3 = -\frac{6}{m\,f}\,\frac{(1-\nu_m)\,(1+a)}{\left[1+\frac{1}{4}\nu_m - \frac{3}{2}\frac{G_m}{E_f}(1+\nu_f)\nu_f\right]} \qquad (3c)$$

The maximum axial stress at the center of the inclusion is then:

$$\sigma^f_{xx}(L/2) = \sigma^f_{max} = \frac{K_2\sigma}{K_1}\left[1 - \mathrm{sech}\sqrt{K_1}\frac{L}{2}\right] \qquad (4)$$

For a very long inclusion ($L\to\infty$) this becomes $\sigma^f_{xx}(\infty) = \sigma^f_{\infty} = K_2\sigma/K_1$.

This formulation was verified through numerical analyses which indicate that the shear-lag predicts accurately (within 5%) the axial stresses at the inclusion centerline, for a wide range of material properties and geometries.

3 RESULTS

The proposed shear lag analysis derives the axial inclusion stress (σ^f_{xx}) and interface tractions (σ^i_{xy}, σ^i_{yy}) as linear functions of the exterior soil stresses (σ_1, σ_3). The load-transfer is affected by both material properties (E_f/G_m, ν_f, ν_m) and geometry (f, m, L). Figure 2 presents distributions of σ^f_{xx}, σ^i_{xy}, and σ^i_{yy} (normalized by the major principal stress, σ_1), for inclusions with half lengths, L/2=0.25, 0.5 and 1.5 m, at an external stress ratio, σ_1/σ_3=6. These conditions correspond to a mobilized friction, ϕ=46°, and represent conditions close to failure for plane strain shearing of an unreinforced specimen of medium-dense sand. The calculations assume typical/representative values for the material properties, spacing and thickness of reinforcement.

The results show the following:

1) There are two distinct regions which characterize the soil-reinforcement interaction: I) the zone close to the tip of the inclusion, in which the axial stress (σ^f_{xx}) accumulates ('builds up'), due to the development of

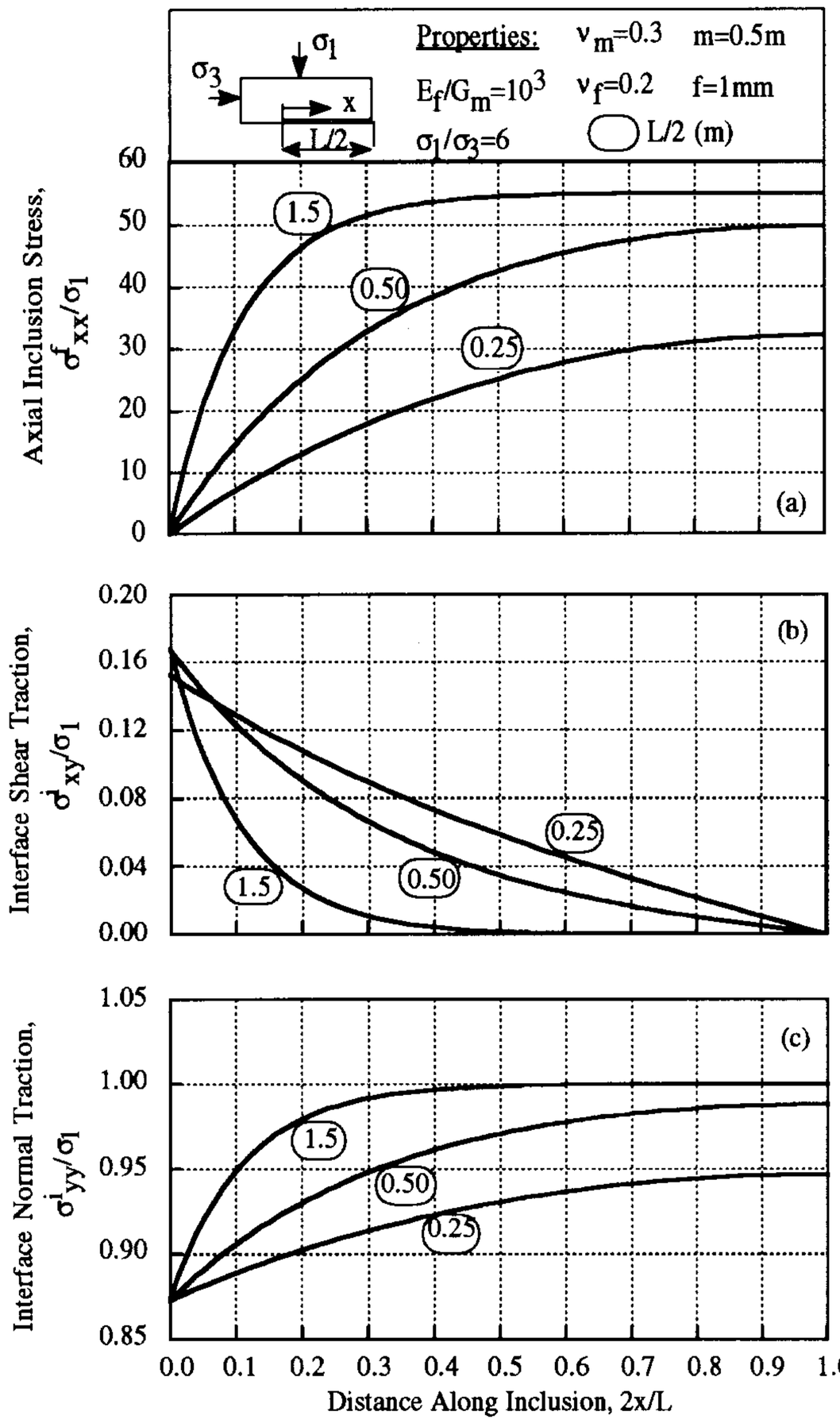

Fig 2 Effect of inclusion length on axial stresses and interface tractions

interface shear stresses (σ^i_{xy}); and II) the zone of constant axial inclusion stress (i.e., $\sigma^f_{xx}\rightarrow\sigma^f_\infty$) where there are no shear tractions at the soil-reinforcement interface. These two regions are fully developed for 'long' inclusions (e.g., L/2=1.5m). However, for short inclusions (L/2=0.25, 0.5m), maximum load transfer is not achieved, and there are gradients of the interface shear tractions occurring at the center of the inclusion (i.e., $d\sigma^i_{xy}/dx<0$ at 2x/L=1).

2) The shear lag parameter, K_1 (eqn. 3a) controls the distribution of axial stress in the inclusion in zone I, while $K_2\sigma/K_1$ determines the maximum load transfer in zone II.

3) Maximum interface shear tractions occur at the tip of the inclusion (Fig. 2b), while $\sigma^i_{xy}=0$ at 2x/L=1 due to symmetry. Figure 2c shows that the interface normal tractions $\sigma^i_{yy}/\sigma_1<1$ throughout zone I and reaches a minimum value at the tip of the inclusion. The ratio $\sigma^i_{xy}/\sigma^i_{yy}$ corresponds to the mobilized friction at the interface. In zone II, $\sigma^i_{xy}=0$ and $\sigma^i_{yy}=\sigma_1$, hence no rotations of principal stresses take place in the surrounding soil matrix.

The 'maximum load transfer ratio', $\sigma^f_{max}/\sigma^f_\infty$ (eqn.4) is a convenient parameter for characterizing the length of reinforcement which mobilizes maximum axial stresses in the inclusion L_I (i.e., the length of zone I). The principal factors affecting $\sigma^f_{max}/\sigma^f_\infty$ are the stiffness ratio, E_f/G_m, spacing and thickness of reinforcement (m, f). Figure 3 shows the maximum load transfer ratio as a function of the inclusion length and stiffness ratio of typical soil reinforcements, $10^2\leq E_f/G_m\leq 10^5$.

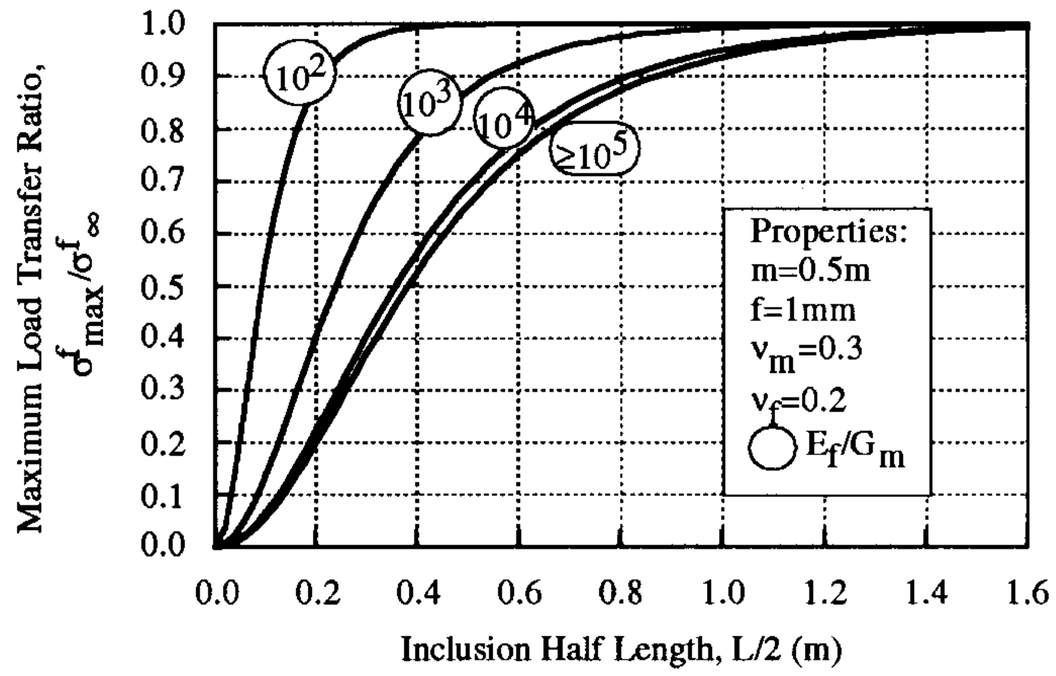

Fig. 3 Effect of inclusion length and stiffness on the maximum load transfer ratio

The pickup length ranges from L_I = 0.8m for a soft inclusion ($E_f/G_m=10^2$) up to 3.2m for stiff reinforcements. The stiffness ratio also affects significantly the load transfer for short inclusions ($L<L_I$, zone I behavior only). These results have important practical implications for the design and interpretation of small scale laboratory tests on reinforced soils (e.g., Whittle et al., 1993).

Figure 4 summarizes reference values of the pickup length, L_I, (defined at $\sigma^f_{max}/\sigma^f_\infty=0.95$), required for maximum load transfer. The results show that L_I increases with stiffness ratio, E_f/G_m, Poisson's ratio in the soil, ν_m, inclusion thickness, f, and spacing, m. For closely spaced reinforcements (m=0.2m), full load transfer can develop for $L_I\leq$ 0.4m, while widely spaced, stiff reinforcements (m=2.0m, $E_f/G_m>10^4$; Fig. 4b) accumulate axial stress for lengths, $L_I>$ 3m. The inclusion thickness affects load transfer mainly for low stiffness ratios ($E_f/G_m\leq 10^3$), while ν_m is only significant for stiff reinforcements ($E_f/G_m\geq 10^4$).

Equation 1 relates the average lateral stress, $\bar{\sigma}^m_{xx}$, in the soil matrix, to the external lateral stress, σ_3, and the reinforcement stress, $\sigma^f_{xx}\rightarrow\sigma^f_\infty$. Thus, the mobilized stress ratio within the reinforced soil

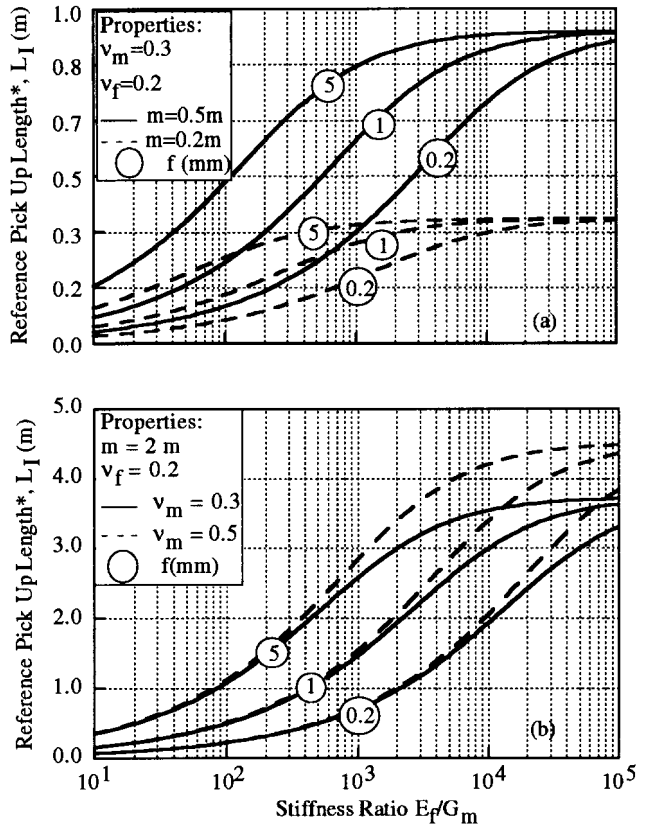

* Defined at $\sigma^f_{max}/\sigma^f_{\infty}$=0.95

Fig. 4 Reinforcement length required for maximum load transfer

matrix, $\sigma_1/\bar{\sigma}^m_{xx}$, can be written:

$$\frac{\sigma_1}{\bar{\sigma}^m_{xx}} = \left(\frac{\sigma_1}{\sigma_3}\right)\left[1 + a\left(1 + \frac{\sigma^f_{\infty}}{\sigma_3}\right)\right]^{-1} \qquad (5)$$

Figure 5 compares the effectiveness of the reinforcement at an external stress ratio, σ_1/σ_3=6. In all cases, the reinforcement reduces the mobilized stress ratio in the soil (i.e., $\sigma_1/\bar{\sigma}^m_{xx}$<6), and is highly effective (i.e., $\sigma_1/\bar{\sigma}^m_{xx} \rightarrow 1/K_0$) for closely spaced (large f/m), stiffer inclusions (large E_f/G_m).

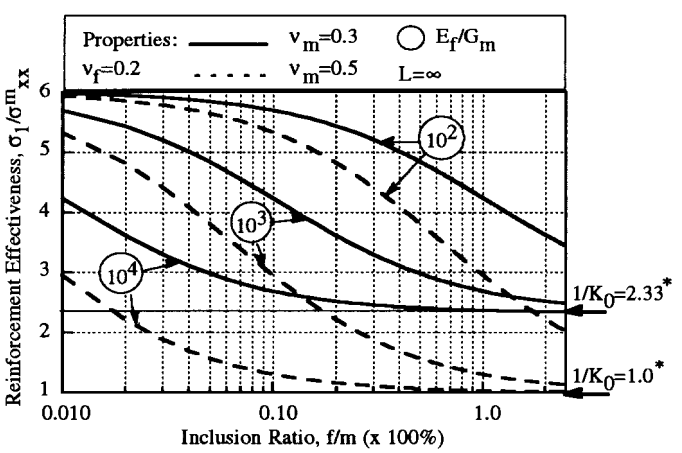

*Note: for elastic soil matrix, $K_0=\nu/(1-\nu)$

Fig. 5 Effectiveness of reinforcements

4 CONCLUSIONS

The mechanism of soil reinforcement using planar inclusions relies on the development of tensile stresses within the reinforcing material. This paper considers the load transfer for a single reinforcement, due to plane strain compression shearing of the surrounding soil matrix. Closed form expressions for the reinforcement stresses are then derived using shear lag approximations and assuming elastic properties for the soil matrix and reinforcing material. The results confirm that stiff, closely spaced reinforcements are most effective in reinforcing the soil mass, provided they are long enough for complete development of axial stresses. The results enable comparisons of the effectiveness of different reinforcements and provide important practical guidance for the design and interpretation of small scale experiments on reinforced soil (e.g., Whittle et al., 1993). Abramento and Whittle (1994a, b) have applied similar shear-lag assumptions to analyze and interpret pullout tests for extensible, planar reinforcements.

REFERENCES

Abramento, M. and Whittle, A.J. (1993) Shear-Lag Analysis of a Planar Soil Reinforcement in Plane Strain Compression, *ASCE Journal of Engineering Mechanics*, 119(2), 270-291.

Abramento, M. and Whittle, A. J. (1994-a) Analysis of Pullout Tests for Planar Reinforcements in Soil, to appear, *ASCE Journal of Geotechnical Engineering*.

Abramento, M. and Whittle, A. J. (1994-b) Experimental Evaluation of Pullout Analyses for Planar Soil Reinforcements, to appear, *ASCE Journal of Geotechnical Engineering*.

Budiansky, B., Hutchinson, J. W. and Evans, A. G. (1986) Matrix Fracture in Fiber-Reinforced Ceramics, *Journal of the Mechanics and Physics of Solids*, 34(2), 167-189.

Harrison, W. J. & Gerrard, C. M. (1972) Elastic Theory Applied to Reinforced Earth, *ASCE Journal of the Soil Mechanics and Foundation Engineering Division*, 98(12), 1325-1344.

Jewell, R. A. (1990) Strength and Deformation in Reinforced Soil Design, *Proc. 4th Intl. Conf. on Geotextiles, Geomembranes and Related Products*, The Hague.

Kuhn, P. (1956) *Stresses in Aircraft and Shell Structures*, McGraw-Hill, 435 pp.

Whittle, A. J.; Larson, D. G.; Germaine, J. T. and Abramento, M. (1993) A New Device for Evaluating Load-Transfer in Geosynthetic Reinforced Soils, *Geosynthetic Soil Reinforcement Testing Procedures*, ASTM STP 1190, S. C. Jonathan Cheng, Ed., American Society for Testing and Materials, Philadelphia, 1-19.